AJNR

Neuroradiologic-Pathologic Correlation in a Neurenteric Cyst of the Clivus

Vibhu Kapoor, Douglas R. Johnson, Melanie B. Fukui, William E. Rothfus and Hae D. Jho

Case Report

Neuroradiologic-Pathologic Correlation in a Neurenteric Cyst of the Clivus

Vibhu Kapoor, Douglas R. Johnson, Melanie B. Fukui, William E. Rothfus, Hae D. Jho

Summary: A 28-year-old woman presented with left-sided frontotemporal headache lasting 6 wk. Head CT and MR imaging revealed a clival mass, which was interpreted as a chondrosarcoma. The lesion was removed at endoscopic endonasal surgery; histologic and immunohistochemical findings proved it to be neurenteric cyst. On CT scans, the lesion was lytic, with an intact cortex; it was uniformly hyperintense relative to gray matter on T1-weighted MR images and iso- to hypointense relative to CSF on T2-weighted MR images.

Neurenteric cysts are developmental lesions resulting from dysgenesis of the notochord and/or neurenteric canal during early embryonic development (1, 2). These cysts are similar to Rathke cleft cysts and colloid cysts at histologic and immunochemical analysis (3, 4). The location of these lesions on images is an important distinguishing feature. A Rathke cleft cyst is usually sellar or suprasellar, whereas a colloid cyst is related to the anterior wall of the third ventricle adjacent to foramen of Monro. Neurenteric cysts have been reported in the cervical, thoracic, and lumbar portions of the spinal canal (1, 5–7); the posterior cranial fossa (1, 8–10); the suprasellar cistern (3); and the anterior cranial fossa (11). We report a case of an intraosseous neurenteric cyst in the clivus.

Case Report

A 28-year-old woman presented with left-sided frontotemporal headache lasting 6 wk. Neurologic findings were normal, and screening CT of the head and sinuses was performed. CT scans of the head revealed a 3 × 2-cm hypoattenuating noncalcified mass in the clivus (Fig, A). The lesion extended superiorly to the dorsum sella, with cortical thinning. On subsequent MR images, the clival mass was well defined, and hyperintensity relative to the gray matter on T1-weighted (TR/TE, 500/14) images (Fig, B) was not suppressed with fat saturation. The lesion was iso- to hypointense relative to CSF on T2-weighted (6000/98) images (Fig, C) and hyperintense relative to gray matter on fluid-attenuated inversion recovery, or FLAIR, (TR/TE/TI, 10,002/157/2200) images. (Because of the

high signal intensity of the lesion on T1-weighted images, contrast enhancement did not add to the diagnosis.) The high signal intensity of the lesion on the T2-weighted images suggested the possibility of a chondroid lesion.

Thereafter, the patient underwent endoscopic endonasal resection of the tumor via the right nostril. At surgery, the tumor was cystic and covered by a thin shell of clival bone at its anterior aspect. It had muddy, gelatinous contents, and total tumor resection was achieved without disruption of the wall of the cyst. The surrounding bone had been remodeled by the mass.

At gross pathologic examination, the mass was a red-tan, collapsed, thin-walled cyst measuring 1.8 × 0.9 × 0.5 cm. Histologic analysis revealed a fibrotic cyst lined by a pseudostratified columnar epithelium with prominent cilia (Fig, D). Focal goblet cells (Fig, D) were intermittently present within the epithelial lining. The mucin content of the goblet cells was positive at periodic acid-Schiff staining with diastase (PASD) (Fig, D), and it was also highlighted with a mucicarmine stain. An immunohistochemical stain for epithelial membrane antigen (EMA) demonstrated strong positive results within the lining epithelium (Fig, E), while an immunohistochemical stain for monoclonal carcinoembryonic antigen (CEA) showed focal positive cytoplasmic findings (Fig, F). A Ki-67 immunohistochemical proliferative index marker showed a low proliferative rate, and both S-100 protein and glial fibrillary acidic protein immunostains were negative. Biochemical analysis was not performed with the contents of the cyst. These findings were interpreted as being most consistent with those of a neurenteric cyst.

The patient underwent follow-up MR imaging 1 y after the surgery (Fig, G). The anterior wall of the clivus showed evidence of prior surgery, but no residual or recurrence of the cyst was present. Clinically, the patient still had headaches, although they were less frequent.

Discussion

Neurenteric cysts result from notochordal dysgenesis during early embryonal development. They are believed to arise from the developing endodermal and notochordal tissues, and they may represent persistence of the neurenteric canal (1, 2). The desmocranium (blastemal skull) starts to form around the developing brain with condensation of the mesenchyme by the end of the first month of embryonic development (2). The occipital plate is first to appear, and it eventually forms the basilar part of the occipital bone. This then extends laterally to surround the hypoglossal nerves on either side, proceeding further ventrally in the midline and dorsal to the pharynx to reach the developing hypophysis. At the same time, the notochord obliquely traverses the occipital plate (Fig, H). At first, it lies near its dorsal surface and then it moves ventrally, where it comes close to the epithelium of the dorsal wall of the pharynx to form
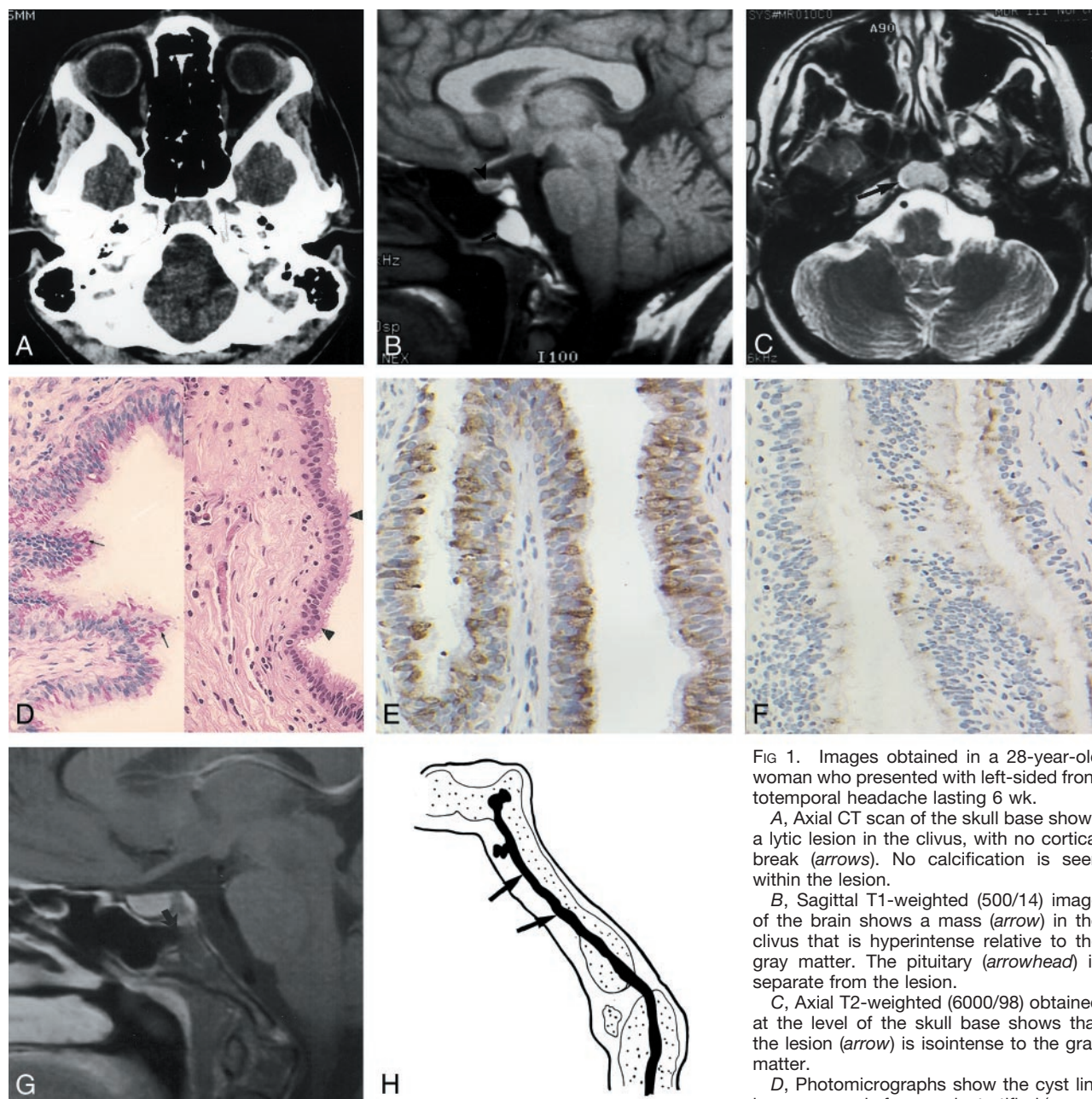
FIG 1. Images obtained in a 28-year-old woman who presented with left-sided frontotemporal headache lasting 6 wk.

A, Axial CT scan of the skull base shows a lytic lesion in the clivus, with no cortical break (*arrows*). No calcification is seen within the lesion.

B, Sagittal T1-weighted (500/14) image of the brain shows a mass (*arrow*) in the clivus that is hyperintense relative to the gray matter. The pituitary (*arrowhead*) is separate from the lesion.

C, Axial T2-weighted (6000/98) obtained at the level of the skull base shows that the lesion (*arrow*) is isointense to the gray matter.

D, Photomicrographs show the cyst lining composed of a pseudostratified (*arrowheads*) ciliated columnar epithelium (*right image*; hematoxylin-eosin, original magnification ×100) and cytoplasmic mucin and Goblet cells (*arrows* in *left image*; PASD, original magnification ×100).

E, Photomicrograph shows strong positive immunohistochemical staining within the lining epithelium (EMA, original magnification ×200).

F, Photomicrograph shows focal positive immunohistochemical staining within the lining epithelium (monoclonal CEA, original magnification ×200).

G, Sagittal contrast-enhanced T1-weighted brain MR (615/12) image obtained at 1-y follow-up shows a typical surgical defect in the anterior wall of the clivus (*arrow*), with no recurrence of the cyst.

H, Sagittal view through the clivus at approximately 3 wk of embryonic development shows the notochord (*arrows*), which obliquely traverses the occipital plate.

the posterior wall of the pharynx. Transiently, it fuses with the dorsal wall of the pharynx and then reenters the cranial base and courses ventrally to end just caudal to the hypophysis (2). Hence, the notochord could conceivably carry some of the endodermal elements with it as it invaginates into the clivus.

Neurenteric cysts, colloid cysts, and Rathke cleft cysts are similar at histologic and immunochemical analysis, and their locations are important distinguishing features (3). A Rathke cleft cyst is sellar or suprasellar, a neurenteric cyst usually is in the posterior fossa, and a colloid cyst typically is in the region of the foramen of Monro along the anterior superior wall of the third ventricle. In a study involving nine cases of neurenteric cysts (1), the most common location was intraspinal, with the cervical region being

the most common intraspinal site. Associated vertebral anomalies were present in six of the seven cases of intraspinal neurenteric cysts (1). These anomalies mainly consisted of segmentation fusion defects, specifically anterior spina bifida, which should suggest the possibility of a neurenteric cyst. Aoki et al (6) and Woo et al (12) divided spinal neurenteric cysts into two types: type I developmental neurenteric cysts that typically are in the cervical region anterior to the cord and without associated spinal defects and type II or III cysts (also called teratomatous cysts) at the level of the conus, posterior to the cord or roots, that are frequently associated with spinal defects. These cysts can be intramedullary, where they are difficult to treat and may recur (2, 3). Intracranial neurenteric cysts also have been described in the cerebellopontine angle cistern (1, 8–10), prepontine cistern (8, 13), suprasellar cistern (3), and anterior cranial fossa (11).

Kimura et al (14) have described the MR imaging of the normal and abnormal clivus well. They retrospectively examined findings in 500 patients and compared the signal intensity of the normal clivus and abnormal clivus with the signal intensity of pons. The signal intensity of the clivus was hypointense relative to that of the pons on T1-weighted images in all patients with an abnormal clivus. On T2-weighted images, the abnormal clivus had varied signal intensity; it was diffusely hypointense to hyperintense relative to the pons. All clival tumors had intense enhancement in this study. Normal clivus can be enhancing to some degree; thus, a hypointense tumor can become isointense relative to the normal marrow after the administration of gadopentetate dimeglumine (15). Therefore, a nonenhanced T1-weighted image is more sensitive than a T2-weighted image in depicting marrow disease of the clivus (15). The most common lesions in the clivus were metastases (eight of 21 cases), and breast carcinoma was the most frequent primary lesion (five of eight cases) (14). On MR images, the signal intensity characteristics of neurenteric cysts reflect the content of the cysts. Proteinaceous cysts without hemorrhage have a variable range of signal intensity, depending on their protein content (7). Hayashi et al (16), in an exhaustive review of the biochemical findings in the contents of Rathke cleft cysts, found that the signal intensity was low on T1-weighted images and high on T2-weighted images with protein concentrations of 10,000 mg/dL or less. With protein concentrations of 10,000–17,000 mg/dL, high signal intensity was present on both T1- and T2-weighted images. With concentrations of 17,000 mg/dL and more, signal intensity was high on T1-weighted images and low on T2-weighted images. The neurenteric cyst in our case had uniformly high signal intensity on T1-weighted images (Fig, B), with varying areas of iso- or hyperintensity relative to gray matter on T2-weighted images (Fig, C). These findings suggest moderate to high concentrations of protein within the cyst in different regions.

The characteristic gross and histologic features of a neurenteric cyst are essentially those of the current case. The cyst wall typically is thin and often partially translucent; these features impart a smooth outer contour to a unilocular cystic cavity, with variable contents. However, focal areas of fibrous thickening may be seen in portions of the cyst wall. Usually, the cyst contains homogeneous material ranging from a serous, clear, watery fluid to a dense, opaque substance resembling colloid. These gross and histologic qualities of neurenteric cysts have led some authors to suggest they, in fact, are related to Rathke cleft cysts and colloid cysts. All three lesions have cellular elements derived from an endodermal (enterogenous) origin (3, 17). They are believed to have a common origin from endodermal remnants (9), and they have also been termed neuroepithelial cysts.

The histologic appearance of these cysts includes a lining epithelium that ranges from nonciliated to ciliated, low cuboidal to columnar (and occasionally stratified columnar epithelium), with a variable number of admixed Goblet cells (3, 9–11, 13, 17, 18). These mucinous features permit overall comparison with the normal respiratory or gastrointestinal tract lining. A thin basement membrane and loose fibrous tissue base usually support the lining epithelium, and focal chronic inflammation may be seen in the cyst wall. Histochemical stains that highlight cytoplasmic mucin include PASD and mucicarmine stains. Additional evidence supporting the endodermal origin of these cysts is largely derived from results of immunohistochemical analysis (3, 9–11, 13, 17, 18). The lining epithelium, as expected, stains positively for most low- and high-molecular-weight cytokeratins (AE1 and AE3, Cam 5.2), EMA, CEA, and vimentin. Positive EMA findings aid in confirming a specific diagnosis of a neurenteric cyst, while CEA results indicate an origin from the gastrointestinal tract (9, 13). Negative staining results usually occur with S-100 protein, a marker for both glial and schwannian differentiation (occasional focal positivity has been reported with neurenteric cysts); glial fibrillary acidic protein (GFAP), a marker of astrocytic, oligodendrocytic, and ependymal differentiation; neuron specific enolase (NSE), a marker of neuroectodermal and neuroendocrine differentiation; and transthyretin (prealbumin), a marker of a normal and neoplastic choroid plexus. Results with these stains are routinely positive in neuroglial and choroid plexus–derived cysts and papillomas (9, 10, 17).

Occasionally enterogenous cysts are disrupted in vivo and undergo degenerative changes, including cyst wall thickening and fibrosis associated with hemorrhage, denudation of the lining epithelium, a xanthogranulomatous histiocytic response, and hemosiderin deposition (10, 17, 18). In this situation, the columnar epithelium could theoretically undergo squamous metaplasia, but diagnostic confusion with epidermoid or dermoid cysts is unlikely given that these two lesions usually have mature keratinized squamous epithelium.

In summary, a neurenteric cyst is an unusual cause for a clival mass. We believe that the presenting symptom (headache) of the patient and the presence of the cyst were incidental. Distinguishing these be-

nign developmental cysts from other clival lesions such as chordoma, chondrosarcoma, metastasis, lymphoma, meningioma, fibrous dysplasia, and infection is important (14, 15). The high signal intensity of a clival mass on T1-weighted images and the lack of enhancement may indicate a benign pathologic condition.

References

1. Brooks BS, Duvall ER, Gammal TE, Garcia JH, Gupta KL, Kapila A. **Neuroimaging features of neurenteric cysts: analysis of nine cases and review of the literature.** *AJNR Am J Neuroradiol* 1993; 14:735–746
2. Williams PL, Warwick R. *Gray's Anatomy* 36th ed. Philadelphia, Pa: W.B. Saunders; 1980;110–141
3. Graziani N, Dufour H, Figarella-Branger D, Donnet A, Bouillot, Grisoli F. **Do the suprasellar neurenteric cyst, the Rathke cleft cyst and the colloid cyst constitute a same entity?** *Acta Neurochir (Wien)* 1995;133:174–180
4. Lach B, Scheithauer BW. **Colloid cyst of the third ventricle: a comparative ultrastructural study of neuraxis cysts and choroid plexus epithelium.** *Ultrastructural Pathol* 1992;16:331–349
5. Pierot L, Dormont D, Oueslati S, Cornu P, Rivierez M, Bories J. **Gadolinium-DTPA enhanced MR imaging of intradural neurenteric cysts.** *J Comput Assist Tomogr* 1988;12:762–764
6. Aoki S, Machida T, Sasaki Y, Yoshikawa K, Iio M, Sasaki T, et al. **Enterogenous cyst of cervical spine : clinical and radiological aspects (including CT and MRI).** *Neuroradiology* 1987;29:291–293
7. Geremia GK, Russell EJ, Clasen RA. **MR imaging characteristics of a neurenteric cyst.** *AJNR Am J Neuroradiol* 1988;9:978–980
8. Malcolm GP, Symon L, Kendall B, Pires M. **Intracranial neurenteric cysts.** *J Neurosurg* 1991;75:115–120
9. Harris CP, Dias MS, Brockmeyer DL, Townsend JJ, Willis BK, Apfelbaum RI. **Neurenteric cysts of the posterior fossa: recognition, management, and embryogenesis.** *Neurosurgery* 1991;29:893–897
10. Eynon-Lewis NJ, Kitchen N, Scaravilli F, Brookes GB. **Neurenteric cyst of the cerebellopontine angle: case report.** *Neurosurgery* 1998; 42:655–658
11. Bevetta S, El-Shunnar K, Hamlyn PJ. **Neurenteric cyst of the anterior cranial fossa.** *Br J Neurosurg* 1996;10:225–227
12. Woo PYC, Sharr MM. **Childhood cervical enterogenous cyst presenting with hemiparesis.** *Postgrad Med J* 1982;58:424–426
13. Simon JA, Olan WJ, Santi M. **Intracranial neurenteric cysts: a differential diagnosis and review.** *Radiographics* 1997;17:1587–1593
14. Kimura F, Kim KS, Friedman H, Russell EJ, Breit R. **MR imaging of the normal and abnormal clivus.** *ANJR Am J Neuroradiol* 1990; 11:1015–1021
15. Chaljub G, Fleet RV, Guinto FC, Crow WN, Martinez L, Kumar R. **MR imaging of clival and paraclival lesions.** *AJR Am J Roentgenol* 1992;159:1069–1074
16. Hayashi Y, Tachibana O, Muramatsu N, et al. **Rathke cleft cyst: MR and biomedical analysis of cyst contents.** *J Comput Assist Tomogr* 1999;23:34–38
17. *Greenfield's Neuropathology* 6th ed. New York, NY: Oxford University Press; 1997;780–786
18. Chaynes P, Bousquet, Sol JC, Delisle MB, Richaud J, Lagarrigue J. **Recurrent intracranial neurenteric cysts.** *Acta Neurochir (Wien)* 1998;140:905–911